

Research Article

An Improved Bingham Model and the Parameter Identification of Coal (Rock) Containing Water Based on the Fractional Calculus Theory

Feng He , Song Yang , Tianjiao Ren , Hongjie Bian , and Haoran Li 

Department of Mechanics and Engineering, Liaoning Technical University, Fuxin 123000, China

Correspondence should be addressed to Song Yang; 2411423170@qq.com

Received 2 December 2021; Accepted 21 December 2021; Published 31 December 2021

Academic Editor: Yonghong Wang

Copyright © 2021 Feng He et al. This is an open access article distributed under the Creative Commons Attribution License, which permits unrestricted use, distribution, and reproduction in any medium, provided the original work is properly cited.

The rheological properties of coal (rock) containing water cannot be characterized by the traditional Bingham model. This problem was addressed in this study through theoretical analysis and experimental research. Based on fractional calculus theory, a fractional calculus soft element was introduced into the traditional Bingham model. An improved Bingham model creep equation and a relaxation equation were obtained through theoretical derivations. Triaxial creep experiments of coal (rock) with different moisture contents were conducted. The parameters of the improved Bingham model were obtained by the least-squares method. Conclusions are as follows: (1) in the improved Bingham model, the stage of nonlinear accelerated creep could be characterized by the creep curves of the soft element; (2) with the increasing moisture content of the coal (rock), the transient strain and the slope of the steady creep stage increased and the total creep time showed a decreasing trend; and (3) the parameters of the creep model were obtained by nonlinear fitting of experimental data, and the fitted curve could better describe the whole creep process. The rationality of the improved creep model was verified. It can provide a theoretical basis for the study and engineering analysis of coal (rock).

1. Introduction

More than 50% of unstable slope and mining failures are related to the creep process caused by groundwater movement [1, 2]. Slope stability evaluation is affected by groundwater movement and temperature effects, which is a popular topic in geological engineering [3, 4]. The waste solution will be discharged into the stratum by the groundwater movement [5, 6]. Likewise, if the moisture content of coal (rock) is excessive, safety and environmental pollution issues will arise. Results of several studies [7–10] have shown that coal (rock) containing water exhibits rheological characteristics [11–13], with creep as the main rheological behaviour [14, 15]. The mechanical properties of coal (rock) will be changed after creep occurs, which will cause deformation and instability of the coal (rock). These are the main factors of major engineering accidents [16]. As a consequence, it is critical

to investigate the creep properties of coal (rock) containing water.

The creep characteristics of coal (rock) containing water have become a popular research topic. As a classic creep model [17–19], the Bingham model can describe the linear creep stage of coal (rock). However, it cannot represent the nonlinear stage of creep. Furthermore, many properties of the nonlinear creep of coal (rock) are not fully understood, and its research methods are also limited [20]. Mandelbrot [21] found that fractal phenomena can be described by fractional calculus. The creep of an object between an ideal solid [22–24] and fluid [25–27] is also a fractal phenomenon. Based on the moisture content, coal (rock) can show rigid, plastic, soft, and flow states. Thus, coal (rock) containing water can be considered to be an object between an ideal solid and fluid.

Many scholars have performed considerable work on creep models. Liu [28] first introduced fractional calculus

theory and combined it with the generalized Maxwell model and the Voigt model in 1994. He used the Laplace transform algorithm [29, 30] to obtain the stress relaxation equation of a non-Newtonian fluid and the approximate analytical solution for the creep behaviour. This is the first time that scholars combined fractional calculus theory with a creep model. Zhang [31] combined the theory of fractional calculus and the classical model and derived constitutive equations for the model. Yin [32] used the fractional calculus theory of Riemann and Liouville [33] to model a soft element and determine its constitutive equation. Pavlyuk [34] considered the problem of stress relaxation of nonlinear viscoelastic materials under unsteady deformation conditions and water movement. To describe the deformation process and temperature effect, a nonlinear creep model of the Rabotnov type [35–37] with a time-independent nonlinearity was used.

The issue of the inadequate description of nonlinear rheological behaviour has been solved by previous research to a certain extent, but there are still errors in the calculation accuracy. There are few examples of fractional calculus theory being applied to creep. Therefore, this paper introduces soft elements based on the fractional calculus theory and the Bingham model. In order to describe the nonlinear stage of creep, an improved Bingham creep model is proposed. Riemann–Liouville fractional calculus was used to derive a creep equation and a relaxation equation. Triaxial creep experiments on coal (rock) with different moisture contents were carried out, and the rationality of the improved creep model was verified through parameter identification. The proposed equations can be used to establish a theoretical foundation for the study and engineering analysis of coal (rock).

2. Bingham Model

The conventional Bingham model [38, 39] is made up of a Hooke body and an elastic viscoplastic body in series. The mechanical model is shown in Figure 1. The constitutive equations are as follows:

$$\begin{aligned} \sigma < \sigma_s, \quad \sigma &= E\varepsilon, \\ \dot{\sigma} &= E\dot{\varepsilon}, \\ \sigma \geq \sigma_s, \quad \eta\dot{\sigma} + E(\sigma - \sigma_s) &= E\eta\dot{\varepsilon}, \end{aligned} \quad (1)$$

where σ and ε are the stress and strain, respectively, $\dot{\sigma}$ and $\dot{\varepsilon}$ are the rates of stress and strain, respectively, σ_s is the yield stress, E is the elastic modulus, and η is the viscosity coefficient.

3. Fractional Calculus Theory

3.1. Fractional Calculus. Riemann–Liouville fractional calculus [33] is the earliest defined and most complete fractional calculus. The integral of order α of a function $f(x)$ is defined as follows:

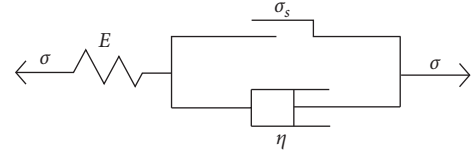


FIGURE 1: Conventional Bingham model.

$$\frac{d^{-\alpha}[f(x)]}{dx^{-\alpha}} = {}_{x_0}D_x^{-\alpha}f(x) = \frac{1}{\Gamma(\alpha)} \int_{x_0}^x (x-t)^{\alpha-1} f(t) dt. \quad (2)$$

The fractional derivative is defined as follows:

$$\begin{aligned} \frac{d^\alpha[f(x)]}{dx^\alpha} &= {}_{x_0}D_x^\alpha f(x) \\ &= \frac{d^m}{dx^m} ({}_{x_0}D_x^{-(m-\alpha)} f(x)) \\ &= \frac{1}{\Gamma(m-\alpha)} \frac{d^m}{dx^m} \left[\int_{x_0}^x \frac{f(t)}{(x-t)^{\alpha-m+1}} dt \right]. \end{aligned} \quad (3)$$

The lower left and lower right indices of D indicate the range of integration, α is the order number of the fractional calculus ($0 < \alpha$, $m-1 < \alpha < m$, $m \in N^*$), and Γ is the Gamma function, where $\Gamma(z) = \int_0^\infty t^{z-1} e^{-t} dt = 2 \int_0^\infty t^{2z-1} e^{-t^2} dt$, $\Gamma(1/2) = 2 \int_0^\infty e^{-t^2} dt = \sqrt{\pi}$, $\Gamma(1+z) = z\Gamma(z)$ ($z \in N^*$), and $\text{Re}(z) > 0$.

The Laplace transform formulas for fractional calculus are as follows:

$$\begin{cases} L[{}_0D_t^{-\alpha} D_t^{-\alpha} f(t), i] = i^{-\alpha} \bar{f}(i) (\alpha > 0), \\ L[{}_0D_t^\alpha f(t), i] = i^\alpha \bar{f}(i) (0 \leq \alpha \leq 1), \end{cases} \quad (4)$$

where the Laplace transform of $f(t)$ is denoted as $\bar{f}(i)$.

3.2. Fractional Soft Element. The state of an object is assumed to be between an ideal solid and fluid. The relationship between the stress and strain is expressed by a fractional derivative, and this object is referred to as a fractional soft element [32]. The mechanical model is shown in Figure 2.

The constitutive equation of the fractional soft element is as follows:

$$\sigma(t) = \xi \frac{d^\alpha \varepsilon(t)}{dt^\alpha}, \quad (0 < \alpha, m \leq \alpha \leq m+1, m \in N^*), \quad (5)$$

where ξ is the inherent coefficient of the soft component.

When $\alpha = 1$ and $\sigma(t) = \xi \cdot \dot{\varepsilon}(t)$, $\dot{\varepsilon}(t)$ is the rates of strain, and the soft element is equivalent to a damper element, which represents an ideal fluid. When $\alpha = 0$ and $\sigma(t) = \xi \cdot \varepsilon(t)$, the soft element is equivalent to a spring element, which represents an ideal solid.

When $\sigma(t) = \text{const}$, the soft element describes the creep behaviour under the condition of a constant stress. Equation (5) is integrated according to the Riemann–Liouville fractional calculus theory, and the creep equation of the soft element can be calculated as follows:

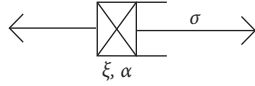


FIGURE 2: Fractional soft element.

$$\varepsilon(t) = \frac{\sigma}{\xi} \frac{t^\alpha}{\Gamma(1 + \alpha)}, \quad (0 < \alpha, m < \alpha < m + 1, m \in N^*). \quad (6)$$

The gamma function values for different α values were calculated by Maple [40]:

$$\text{When } \alpha = 0.1, \quad \Gamma(1 + \alpha) = \Gamma(1.1) = \int_0^\infty t^{0.1} e^{-t} dt = 0.95135$$

$$\text{When } \alpha = 0.3, \quad \Gamma(1 + \alpha) = \Gamma(1.3) = \int_0^\infty t^{0.3} e^{-t} dt = 0.89747$$

$$\text{When } \alpha = 0.5, \quad \Gamma(1 + \alpha) = \Gamma(1.5) = \int_0^\infty t^{0.5} e^{-t} dt = 0.88622$$

$$\text{When } \alpha = 0.7, \quad \Gamma(1 + \alpha) = \Gamma(1.7) = \int_0^\infty t^{0.7} e^{-t} dt = 0.90863$$

$$\text{When } \alpha = 0.9, \quad \Gamma(1 + \alpha) = \Gamma(1.9) = \int_0^\infty t^{0.9} e^{-t} dt = 0.96176$$

The creep curves for different α values asre plotted according to (6), as shown in Figure 3. The strain of the fractional soft element showed a slow upward trend over time [41]. It does not preserve the linear rise of an ideal fluid, nor does the strain remain constant as it does for an ideal solid. The soft element can reflect the nonlinear gradient process of the strain.

Similarly, when $\varepsilon(t) = \text{const}$, a fractional soft element will describe the stress relaxation of creep motion. The relaxation equation of soft element can be derived as follows:

$$\sigma(t) = \varepsilon \cdot \xi \frac{t^{-\alpha}}{\Gamma(1 - \alpha)}, \quad m < \alpha < m + 1, m \in N^*. \quad (7)$$

The Gamma function for different values of α was calculated by Maple [40]:

$$\text{When } \alpha = 0.1, \quad \Gamma(1 - \alpha) = \Gamma(0.9) = \int_0^\infty t^{-0.1} e^{-t} dt = 1.06861$$

$$\text{When } \alpha = 0.3, \quad \Gamma(1 - \alpha) = \Gamma(0.7) = \int_0^\infty t^{-0.3} e^{-t} dt = 1.29805$$

$$\text{When } \alpha = 0.5, \quad \Gamma(1 - \alpha) = \Gamma(0.5) = \int_0^\infty t^{-0.5} e^{-t} dt = 1.77245$$

$$\text{When } \alpha = 0.7, \quad \Gamma(1 - \alpha) = \Gamma(0.3) = \int_0^\infty t^{-0.7} e^{-t} dt = 2.99156$$

$$\text{When } \alpha = 0.9, \quad \Gamma(1 - \alpha) = \Gamma(0.1) = \int_0^\infty t^{-0.9} e^{-t} dt = 9.51350$$

For a constant strain and various α values, the stress relaxation curves obtained by (7) are shown in Figure 4. With the increase in α , the stress gradually approaches 0. The soft element becomes a Hooke body. As α decreases, the stress gradually decreases and finally reaches a stable value. The soft element becomes a viscous fluid. Thus, the soft element is a multicharacteristic element, and the strain rate and stress can be controlled. Traditionally, the strain rate can

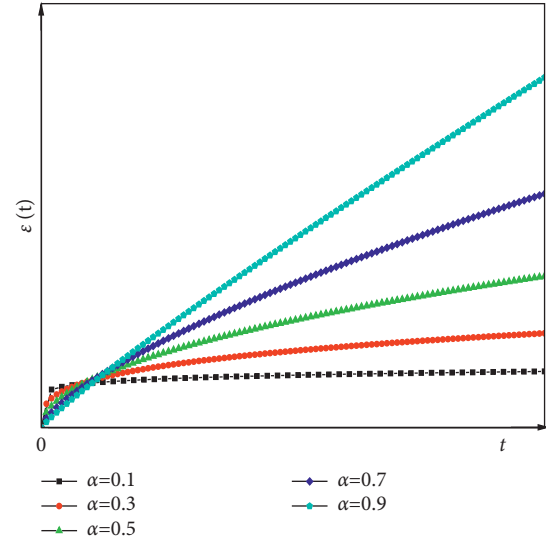


FIGURE 3: Creep curves of fractional soft component under different α .

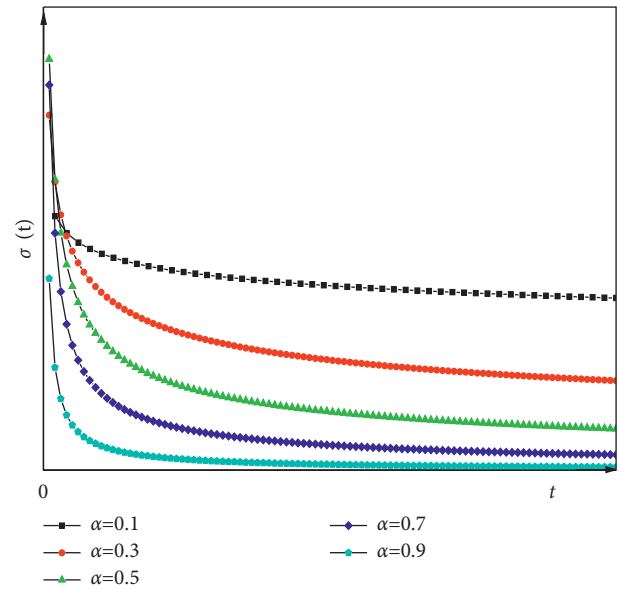


FIGURE 4: Stress relaxation curves of fractional soft component under different values of α .

only be controlled by the viscosity coefficient of the plastic element. The introduction of a soft element into the Bingham model better reflects nonlinear creep behaviour.

4. Improved Bingham Model

To make up for the shortcomings of the traditional Bingham model, the fractional soft element is introduced. The fractional soft element is connected with the Bingham model to form an improved Bingham model. As shown in Figure 5, there are four elements of this model, labelled 1-4 from left to right. The classic creep curve is shown in Figure 6. The whole creep process is divided into three stages: primary creep, steady creep, and accelerated creep.

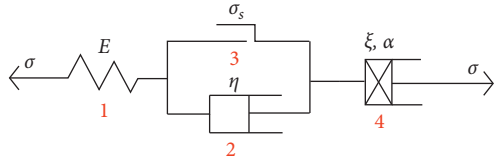


FIGURE 5: Improved Bingham model.

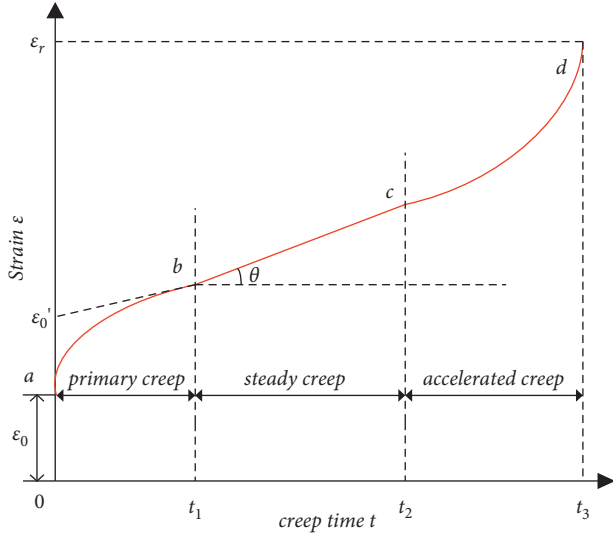


FIGURE 6: Classical creep curve.

The improved creep model satisfies the following conditions:

- (1) When $0 < \sigma < \sigma_s$, the model is equivalent to the Hooke body and the fractional soft element connected in series. The stress of the coal (rock) has not reached its yield strength, and the deformation is in the primary creep period ($0 \rightarrow t_1$). According to the principle of elements in series, the stress of each element is the same, and the total strain of the model is equal to the sum of the strain of each element. The following constitutive equation of the improved creep model can be obtained based on equation (6):

$$\varepsilon(t) = \frac{\sigma}{E} + \frac{\sigma}{\xi_1} \frac{t^{\alpha_1}}{\Gamma(1 + \alpha_1)}, \quad (8)$$

where σ is the initial stress and E is the elastic modulus.

- (2) When $\sigma \geq \sigma_s$, all parts of the model are involved in the creep. The fractional soft element is connected with the traditional Bingham model. The creep reaches the stage of steady creep and accelerated creep ($t_1 \rightarrow t_3$). Based on equation (6), the constitutive equation of the improved creep model is as follows:

$$\varepsilon(t) = \frac{\sigma}{E} + \frac{\sigma - \sigma_s}{\eta} t + \frac{\sigma}{\xi_2} \frac{t^{\alpha_2}}{\Gamma(1 + \alpha_2)}. \quad (9)$$

Combined with (8) and (9), the total expression of the fractional creep model is as follows:

$$\varepsilon(t) = \begin{cases} \frac{\sigma}{E} + \frac{\sigma}{\xi_1} \frac{t^{\alpha_1}}{\Gamma(1 + \alpha_1)}, & (\sigma < \sigma_s), \\ \frac{\sigma}{E} + \frac{\sigma - \sigma_s}{\eta} t + \frac{\sigma}{\xi_2} \frac{t^{\alpha_2}}{\Gamma(1 + \alpha_2)}, & (\sigma \geq \sigma_s). \end{cases} \quad (10)$$

5. Parameter Identification

To verify the rationality of the improved creep model, parameter identification of the model was carried out. The traditional Bingham model was used to describe the rheological characteristics. When the initial stress was less than the yield stress, the model had the characteristics of a solid. After the stress exceeded the yield stress, it exhibited the properties of a liquid and generated flow. To test this model, triaxial creep experiments were carried out on coal (rock) with different moisture contents.

The dimensions of the coal (rock) samples were $\varnothing 50 \text{ mm} \times 100 \text{ mm}$, and the average compressive strength of coal (rock) was 3.68 MPa. The testing apparatus was a machine for static oil pressure testing. The equipment and schematic diagrams of the experiment are shown in Figure 7. The axial compression was controlled to 3 MPa. The moisture contents of the coal (rock) after various hydration times are shown in Table 1.

The triaxial creep experiment data curves under different moisture contents are shown in Figure 8. The improved creep model parameters were obtained by the least-squares method. The parameter E was calculated from the transient strain ε_0 . In the primary creep stage, the parameters α_1 and ξ_1 were obtained by nonlinear fitting with the Origin software. The parameter η was obtained by linear fitting in the steady creep stage. For the accelerated creep stage, the same nonlinear fitting method was used to obtain the parameters α_2 and ξ_2 . The creep parameters are shown in Table 2.

As shown in Figures 8 and 9, the transient strains of the coal (rock) samples with moisture contents of 0%, 0.71%, 1.45%, 1.83%, and 3.67% were 0.010, 0.024, 0.033, 0.044, and 0.053, respectively. With the increase in the moisture content of the coal (rock), the transient strain showed an increasing trend. The slope of the curve during the steady creep increased from 0.0001 to 0.0007. The steady creep was accelerated by the increase in the moisture content of coal (rock). The creep time was gradually reduced from 150 min to about 50 min. The total creep time of the coal (rock) showed a decreasing trend. In the accelerated creep stage, the time required for the coal (rock) to enter the nonlinear creep stage was gradually shortened with the increase in the moisture content. The rate of coal (rock) creep was also accelerated by the increase in the moisture content. The overall results showed that the idea of combining coal (rock) and water to model creep was reasonable.

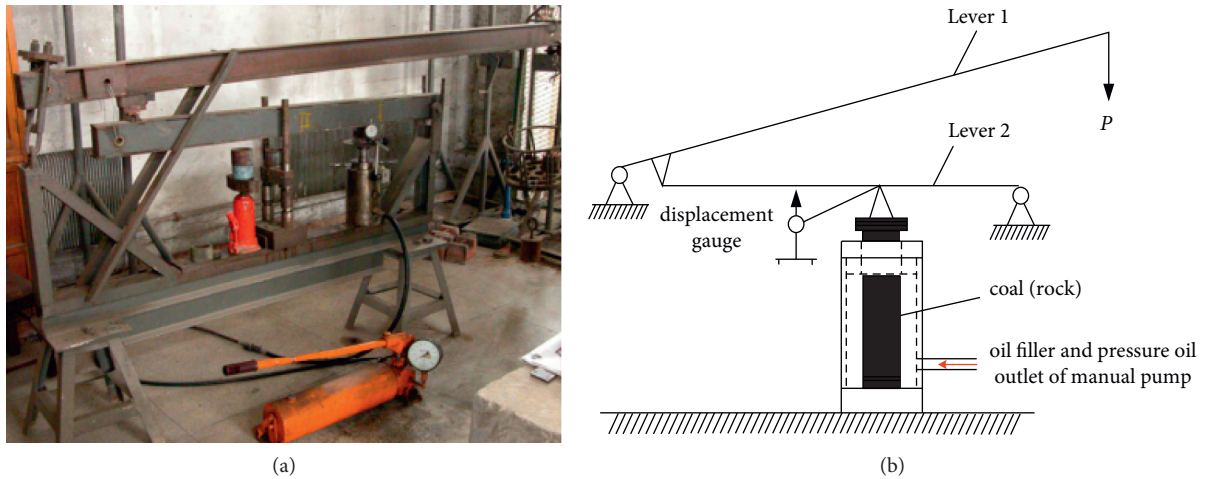


FIGURE 7: Equipment and schematic diagram of the experiment: (a) machine for static oil pressure testing; (b) schematic diagram of the creep test.

TABLE 1: Moisture contents and hydration times.

Moisture content (%)	0	0.71	1.45	1.83	3.67
Hydration time (h)	—	0	12	24	96

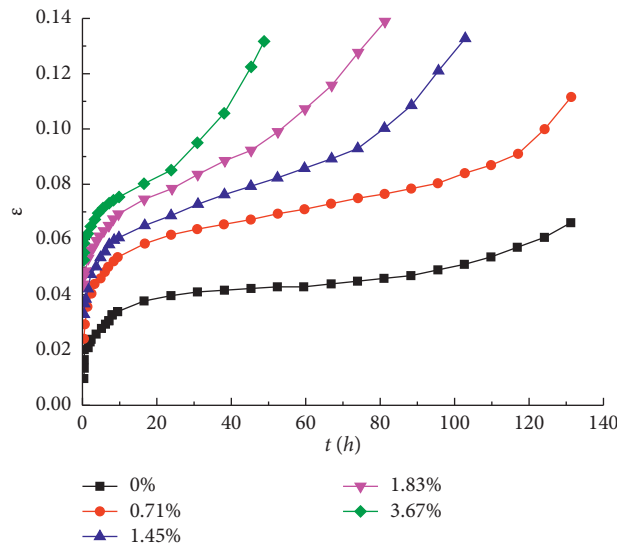
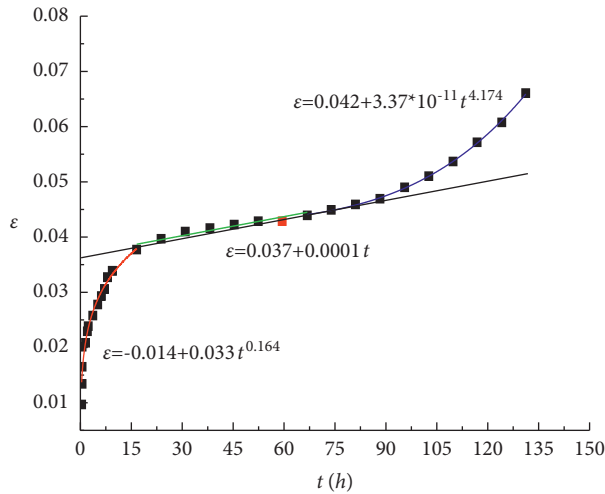


FIGURE 8: Experimental triaxial creep data under different moisture content conditions.

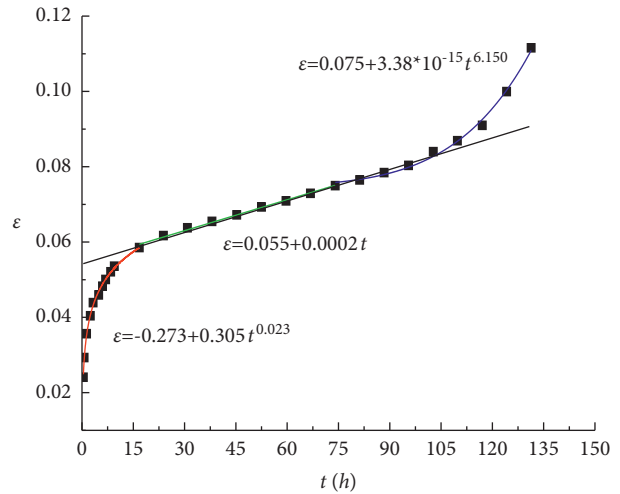
Compared with the fitting curve of the traditional Bingham model, the fitted curve of the improved Bingham model was more consistent with the three stages of coal (rock) creep, especially the nonlinear creep stage. The

primary, steady, and accelerated creep stages followed power function, linear function, and power function trends, respectively. The analytical formulas of the functions are consistent with the established model, and the fitted



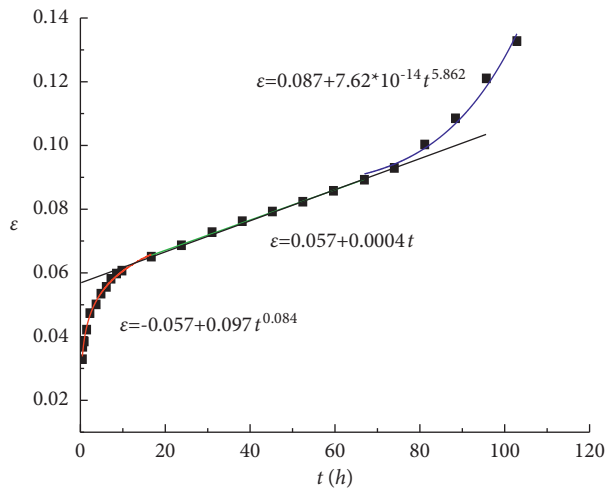
■ experimental data — steady creep
 — primary creep — m
 — accelerated creep

(a)



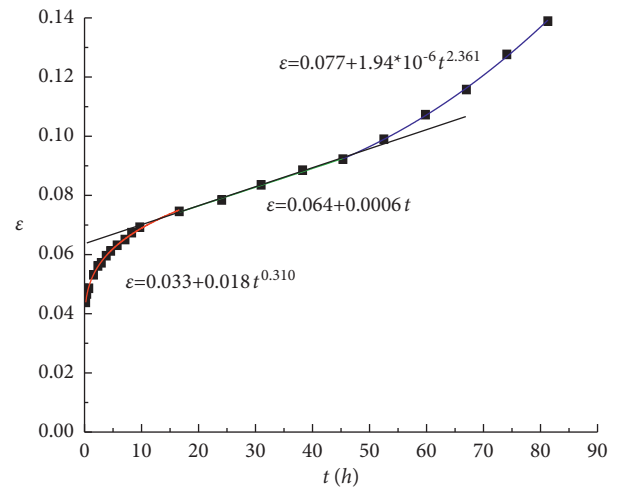
■ experimental data — steady creep
 — primary creep — m
 — accelerated creep

(b)



■ experimental data — steady creep
 — primary creep — m
 — accelerated creep

(c)



■ experimental data — accelerated creep
 — steady creep — m
 — primary creep

(d)

FIGURE 9: Continued.

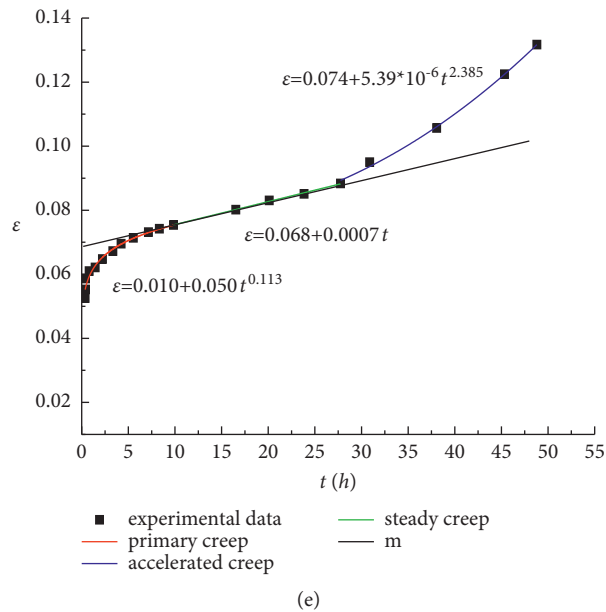


FIGURE 9: Fitting creep curves of coal (rock) with different moisture contents. (a) Fitting curve of coal (rock) with a moisture content of 0%. (b) Fitting curve of coal (rock) with a moisture content of 0.71%. (c) Fitting curve of coal (rock) with a moisture content of 1.45%. (d) Fitting curve of coal (rock) with a moisture content of 1.83%. (e) Fitting curve of coal (rock) with a moisture content of 3.67%.

correlation coefficients were greater than 0.9. In summary, the improved Bingham model is reasonable.

6. Conclusion

- (1) By incorporating a fractional soft element, an improved Bingham model was obtained. Riemann–Liouville fractional calculus theory was used to obtain the creep and relaxation equations of the revised Bingham model.
- (2) The analysis of the experimental data demonstrated that when the moisture content of coal (rock) increased, so did the transient strain and the slope of the steady creep stage, while the overall creep duration decreased. The rate of coal (rock) creep also increased. The overall results indicated that the idea of combining coal (rock) and water to model creep is realistic.
- (3) The least-squares method was used to determine the modified Bingham model parameters based on data from triaxial creep experiments of coal (rock) with various moisture contents. The fitted curve, in particular, the nonlinear creep stage, can characterize the creep stage of coal (rock) containing water. This validated the proposed modified creep model. These results can be used to establish a theoretical foundation for the study and engineering analysis of coal (rock).

Data Availability

The data that support the findings of this study are included in the supplementary material of this article.

Conflicts of Interest

The authors declare that there are no conflicts of interest.

Authors' Contributions

Feng He and Song Yang conceptualized the study. Song Yang developed methodology. Feng He provided software. Song Yang, Tianjiao Ren, and Feng He validated the study. Hongjie Bian and Haoran Li were responsible for formal analysis. Song Yang was responsible for data curation. Feng He prepared the original draft. Song Yang and Haoran Li reviewed and edited the manuscript. Feng He supervised the study. All authors have read and agreed to the published version of the manuscript.

Acknowledgments

This research was funded by National Natural Science Foundation of China, grant no. 51774167.

Supplementary Materials

The original data involved in this paper are shown in the table. (*Supplementary Materials*)

References

- [1] M. Gasc-Barbier, S. Chanchole, and P. Bérest, “Creep behavior of Bure clayey rock,” *Applied Clay Science*, vol. 26, no. 1–4, pp. 449–458, 2003.
- [2] B. Yuan, Z. Li, Z. Zhao, H. Ni, Z. Su, and Z. Li, “Experimental study of displacement field of layered soils surrounding laterally loaded pile based on transparent soil,” *Journal of Soils and Sediments*, vol. 21, no. 9, pp. 3072–3083, 2021.

- [3] B. Yuan, Z. Li, Z. Su, Q. Luo, M. Chen, and Z. Zhao, "Sensitivity of multistage fill slope based on Finite element model," *Advances in Civil Engineering*, vol. 2021, Article ID 6622936, 13 pages, 2021.
- [4] B. Bai, T. Xu, Q. Nie, and P. Li, "Temperature-driven migration of heavy metal Pb²⁺ along with moisture movement in unsaturated soils," *International Journal of Heat and Mass Transfer*, vol. 153, Article ID 119573, 2020.
- [5] B. Bai, Q. Nie, Y. Zhang, X. Wang, and W. Hu, "Cotransport of heavy metals and SiO₂ particles at different temperatures by seepage," *Journal of Hydrology*, vol. 597, Article ID 125771, 2021.
- [6] E. Xue, X. He, B. Nie, and J. He, "Research on the coupling theory of coal-rock rheological electromagnetic radiation," *Coal Science and Technology*, vol. 6, pp. 46–48, 2005.
- [7] B. Bai, G.-C. Yang, T. Li, and G.-S. Yang, "A thermodynamic constitutive model with temperature effect based on particle rearrangement for geomaterials," *Mechanics of Materials*, vol. 139, Article ID 103180, 2019.
- [8] J. F. Shao, Q. Z. Zhu, and K. Su, "Modeling of creep in rock materials in terms of material degradation," *Computers and Geotechnics*, vol. 30, no. 7, pp. 549–555, 2003.
- [9] D. E. Munson, "Constitutive model of creep in rock salt applied to underground room closure," *International Journal of Rock Mechanics and Mining Sciences*, vol. 34, no. 2, pp. 233–247, 1997.
- [10] J. Feng, Z. Chuhan, W. Gang, and W. Guanglun, "Creep modeling in excavation analysis of a high rock slope," *Journal of Geotechnical and Geoenvironmental Engineering*, vol. 129, no. 9, pp. 849–857, 2003.
- [11] W. Yin, Y. Pan, Z. Li, Y. Song, and L. Zhu, "Study on rockburst inoculation process of narrow coal pillar based on rheological properties of coal rock," *Journal of Disaster Prevention and Reduction Engineering*, vol. 36, no. 5, pp. 834–840, 2016.
- [12] B. Bai, D. Rao, T. Chang, and Z. Guo, "A nonlinear attachment-detachment model with adsorption hysteresis for suspension-colloidal transport in porous media," *Journal of Hydrology*, vol. 578, Article ID 124080, 2019.
- [13] K. Zhao, *The Acoustic Emission Characteristics of Creep Failure of Red sandstone in Different Water-Bearing States*, Jiangxi University of Technology, Jiangxi, China, 2021.
- [14] F. Mainardi, E. Masina, and G. Spada, "A generalization of the Becker model in linear viscoelasticity: creep, relaxation and internal friction," *Mechanics of Time-dependent Materials*, vol. 23, no. 3, pp. 283–294, 2019.
- [15] B. Bai, R. Zhou, G. Cai, W. Hu, and G. Yang, "Coupled thermo-hydro-mechanical mechanism in view of the soil particle rearrangement of granular thermodynamics," *Computers and Geotechnics*, vol. 137, no. 8, Article ID 104272, 2021.
- [16] F. He, F. Meng, Z. Wang, and G. Zhao, "Experimental study on effect of water and coal rock creep," *Journal of Liaoning Technical University*, vol. 30, no. 2, pp. 175–177, 2011.
- [17] A. O. Habib, I. Aiad, F. I. El-Hosiny, and A. Mohsen, "Studying the impact of admixtures chemical structure on the rheological properties of silica-fume blended cement pastes using various rheological models," *Ain Shams Engineering Journal*, vol. 12, no. 2, pp. 1583–1594, 2021.
- [18] R. Talat and M. Mustafa, "Bödewadt flow of Bingham fluids over a non-isothermal permeable disk with viscous dissipation effects," *Alexandria Engineering Journal*, vol. 60, no. 3, pp. 2857–2864, 2021.
- [19] J. Xiao, S. Wang, S. Wang, J. Dong, J. Wen, and J. Tu, "Numerical study on forced convection heat transfer across a heated circular tube based on Bingham model with thermally dependent viscosity," *Journal of Heat Transfer*, vol. 143, no. 2, 2021.
- [20] B. Bai, D. Rao, T. Xu, and P. Chen, "SPH-FDM boundary for the analysis of thermal process in homogeneous media with a discontinuous interface," *International Journal of Heat and Mass Transfer*, vol. 117, pp. 517–526, 2018.
- [21] B. B. Mandelbrot and J. A. Wheeler, "The fractal geometry of nature," *American Journal of Physics*, vol. 51, no. 3, pp. 286–287, 1983.
- [22] J. Xu, "An isothermal equation of state (IV) -ideal solid and absolute pressure coordinates," *High pressure physics*, vol. 1, pp. 22–33, 1988.
- [23] Y. Zhou, Y. Chen, and J. Chen, "Fractional Poynting-Thomson rheological model," *Journal of Southwest University of Science and Technology*, vol. 28, no. 1, pp. 31–35, 2013.
- [24] L. S. Castleman, "Ternary diffusion: the (2-D) matrix of an ideal solid solution," *Metallurgical Transactions A*, vol. 14, no. 1, pp. 45–51, 1983.
- [25] A. A. Shiryayev, "Eigenfrequencies of the oscillating surface of a free-falling compound drop of an ideal liquid," *Fluid Dynamics*, vol. 55, no. 3, pp. 291–299, 2020.
- [26] R. V. Akinshin, "New instability of a thin vortex ring in an ideal fluid," *Fluid Dynamics*, vol. 55, no. 1, pp. 74–88, 2020.
- [27] A. N. Guz and A. M. Bagno, "Influence of prestresses on normal waves in an elastic compressible half-space interacting with a layer of a compressible ideal fluid," *International Applied Mechanics*, vol. 55, no. 1-9, pp. 585–595, 2019.
- [28] C. Liu, "Generalized Maxwell model of non-Newtonian fluid and its solution," *Mechanics and practice*, vol. 2, pp. 21–23, 1995.
- [29] Deutsches Institut für Normung E.V. (DIN), DIN 5487, *Fourier-Laplace- and Z-transformation Symbols and Concepts*, Deutsches Institut für Normung E.V. (DIN), Berlin, Germany, 1988.
- [30] V. Eiderman, *An Introduction to Complex Analysis and the Laplace Transform*, CRC Press, Boca Raton, FL, USA, 2021.
- [31] W. Zhang, "A new rheological model theory using fractional derivative," *Journal of Natural Sciences*, Xiangtan University, vol. 1, , pp. 30–36, 2001.
- [32] D. Yin, J. Ren, C. Liang, and C. Wen, "A new geotechnical rheological model element," *Journal of Rock Mechanics and Engineering*, vol. 9, pp. 1899–1903, 2007.
- [33] Y. Luchko, "Fractional derivatives and the fundamental theorem of fractional calculus," *Fractional Calculus and Applied Analysis*, vol. 23, no. 4, pp. 939–966, 2020.
- [34] Y. V. Pavlyuk, "Modeling of the stress relaxation of non-linear viscoelastic materials under unsteady deformation conditions," *Strength of Materials*, vol. 49, no. 5, pp. 652–659, 2017.
- [35] X.-Y. Wang, X. Wang, X.-C. Zhang, and S.-F. Zhu, "Creep damage characterization of UNS N10003 alloy based on a numerical simulation using the Norton creep law and Kachanov-Rabotnov creep damage model," *Nuclear Science and Techniques*, vol. 30, no. 4, p. 65, 2019.
- [36] C. Praveen, J. Christopher, V. Ganesan, G. V. Prasad Reddy, and S. K. Albert, "Prediction of Creep Behaviour of 316LN SS under Uniaxial and Multiaxial Stress State Using Kachanov-Rabotnov Model at 923 K," *Transactions of the Indian Institute of Metals*, vol. 73, pp. 1–9, 2020.
- [37] B. Bai and X. Shi, "Experimental study on the consolidation of saturated silty clay subjected to cyclic thermal loading," *Geomechanics and Engineering*, vol. 12, no. 4, pp. 707–721, 2017.

- [38] N. El Khouja, N. Roquet, and B. Cazacliu, "Analysis of a regularized Bingham model with pressure-dependent yield stress," *Journal of Mathematical Fluid Mechanics*, vol. 17, no. 4, pp. 723–739, 2015.
- [39] B. E. Powers, N. M. Wereley, and Y.-T. Choi, "Analysis of impact loads in a magnetorheological energy absorber using a Bingham plastic model with refined minor loss factors accounting for turbulent transition," *Meccanica*, vol. 51, no. 12, pp. 3043–3054, 2016.
- [40] R. P. Gilbert, G. C. Hsiao, and R. J. Ronkese, *Differential Equations: A Maple™ Supplement*, CRC Press, Boca Raton, FL, USA, 2021.
- [41] B. Yuan, Z. Li, Y. Chen et al., "Mechanical and microstructural properties of recycling granite residual soil reinforced with glass fiber and liquid-modified polyvinyl alcohol polymer," *Chemosphere*, vol. 268, Article ID 131652, 2021.